Materials Advances

Accepted Manuscript

This article can be cited before page numbers have been issued, to do this please use: S. Simon, L. Theresa and P. B. Sreeja, *Mater. Adv.*, 2025, DOI: 10.1039/D4MA01270D.

View Article Online
DOI: 10.1039/D4MA01270D

Unzipped MWCNT/Polypyrrole Hybrid Composites: A Pathway to High-Performance Asymmetric Supercapacitors

Shilpa Simon[a], Letcy V Theresa[a], Sreeja P B[a]*

[a] Department of Chemistry, Christ University, Bengaluru 560029, IN
*Corresponding Author

E-mail: sreeja.pb@christuniversity.in,

https://orcid.org/**0000-0002-2106-7867**

ABSTRACT

A novel method has been developed for the conversion of multi-walled carbon nanotubes (MWCNTs) into unzipped MWCNTs (UzMWCNT) using a modified Hummers method followed by reduction. This technique allows for the controlled modification of MWCNTs in both transverse and longitudinal directions. The UzMWCNT exhibit unique structural characteristics that combine the properties of 1D nanotubes and graphene-like features. The UzMWCNT/PPy composite exhibited an impressive specific capacitance of 944 F g^{-1} along with excellent cycling stability, retaining 92% of its capacitance after 5000 cycles. For the UzMWCNT/PPy//AC composite, the gravimetric capacitance decreased with increasing current density, from 400 F g^{-1} at 1.0 A g^{-1} to 162 F g^{-1} at 2.5 A g^{-1}. Furthermore, the UzMWCNT/PPy//AC composite demonstrated outstanding long-term durability, retaining approximately 95% of its capacitance after 5000 cycles at a current density of 5 A g^{-1}, underscoring its excellent cycling stability. This research paves the way for the development of high-performance supercapacitor electrodes using hybrid materials derived from MWCNTs.

KEYWORDS

Multiwalled carbon nanotubes, Polypyrrole, Unzipping, Supercapacitors, Energy storage

1. INTRODUCTION

To meet the demands of sustainable societal development, researchers are continuously exploring advancements in renewable energy.[1–3] Batteries and supercapacitors represent two of the most promising directions and are widely utilized as energy storage devices.[4–6] Electrochemical capacitors, or supercapacitors, offer significant advantages over traditional batteries, including longer life cycles, rapid power delivery and absorption, high power density, and excellent energy reversibility.[7–11] Due to these features, supercapacitors are becoming a

View Article Online
DOI: 10.1039/D4MA01270D

preferred energy storage solution for various applications, such as hybrid electric vehicles, portable electronics, and energy management systems.[12–14]However, their overall performance is largely determined by the choice of electrode materials, which directly affects the device's capacity, power delivery, and durability.[15–17] Carbon-based materials, in particular, are essential in meeting the growing demand for efficient energy storage solutions.[18–21]

In this context, Carbon nanotubes (CNTs) have emerged as promising candidates for supercapacitor electrodes owing to their well-defined nanostructure, high electrical conductivity, and chemical stability.[22–26] However, conventional CNTs are typical of micrometre-scale lengths and tend to aggregate into tangled bundles, impeding ion transport within the tubes, especially in the case of MWCNTs.[27] Consequently, this limits any significant improvement in the specific capacitance of supercapacitors. To fully harness the exceptional properties of CNTs, methods for macroscopic modification are required.[28–30] MWCNTs exhibit excellent intrinsic conductivity; however, their tubular structure often leads to agglomeration and limited surface accessibility, which can hinder their electrochemical performance.[31–33]

Recent advances in CNT manipulation have led to the production of shorter fragments and nanoribbons through cutting processes.[34] Various techniques have been employed to shorten long CNTs, including ball milling, cryogenic crushing, solid-state reactions, selective etching, fluorination, chemical oxidation, and electrochemical methods.[35–37] Short segments obtained from transverse cutting have demonstrated superior performance in energy applications.[38] Additionally, longitudinal unzipping of CNTs has been achieved through processes like plasma etching, oxidative treatment, electrochemical approaches, potassium vapour treatment, and catalytic hydrogenation.[39–43] Despite these advancements, the one-step cutting and unzipping of CNTs in both directions remains challenging due to complex procedures and intricate manipulation.[38] However, the potential for improved electrochemical reactivity with open-ended CNTs has been observed. Thus, there is a persistent need to develop effective strategies for simultaneously cutting and splitting CNTs.[44] We utilized a cost-efficient, modified Hummers method to process MWCNTs.[45,46] Our results indicate that the MWCNTs were cut transversely and unzipped longitudinally, leading to the formation of curved graphene nanostructures, which may exhibit a structure partially resembling interconnected graphene fragments.

Conductive polymer-CNT exhibit remarkable electrochemical performance when used as supercapacitor electrodes[47]. Among the most promising conductive polymers, researchers have

View Article Online
DOI: 10.1039/D4MA01270D

shown particular interest in polyaniline (PANI),[48] polypyrrole (PPy),[49] polythiophene (PTh),[50] and their modified versions. PPy is notable for its high conductivity, excellent redox reversibility, and eco-friendliness.[51–53] However, it is plagued by issues of swelling and degradation of polymer chains, which result in inadequate cyclic stability.[54,55]

To address these limitations, UzMWCNT has been incorporated into the PPy matrix to enhance the mechanical, thermal, and electrical conductivity of the composites. This improvement arises from the synergistic interactions between the constituent elements. UzMWCNT boast both superior electrical conductivity and mechanical strength, while also promoting efficient charge transport. This translates to speedy charging and discharging capabilities in supercapacitors.[56] Various methods for creating composites of CNTs and conductive polymers such as electrochemical methods[57], Microemulsion polymerization,[58] Vapor-phase polymerization[59], and In-situ polymerization.[60] In-situ polymerization plays a crucial role in the production of conducting polymers and carbon-based materials for supercapacitors.[53–55] This innovative technique allows for the controlled synthesis of polymers and carbon structures directly within the desired application, resulting in enhanced performance and tailored properties.[64,65]

In this study, we employ a modified Hummers method to achieve the cutting and unzipping of CNTs, utilizing cost-effective MWCNTs as raw materials resulting in the formation of UzMWCNT. This report outlines a one-step synthesis method for creating UzMWCNT/PPy composites. The process involves interfacial polymerization of pyrrole conducted within solvents containing UzMWCNT. The primary benefit of utilizing interfacial polymerization for the synthesis of nanocomposite materials, in general, lies in the exceptionally slow reaction rate. This characteristic allows for precise encapsulation of nanostructures like UzMWCNT in this instance, resulting in improved dispersion within the polymer matrix, making it highly promising for supercapacitor applications.

2. Materials and Methods

2.1. Materials

Multi-walled carbon nanotube (MWCNT > 95.0%), Pyrrole (monomer 99.5%), ammonium persulfate (APS, ≥ 98%), Sodium nitrate($NaNO_3$), Sulfuric acid (H_2SO_4), Potassium Permanganate ($KMnO_4$), Hydrogen Peroxide (H_2O_2), Sodium borohydride ($NaBH_4$), Hydrochloric acid (HCl) were purchased from Sigma-Aldrich. All chemicals were high-grade reagents and were used as received.

View Article Online
DOI: 10.1039/D4MA01270D

2.2. UzMWCNT/PPy

The synthesis of UzMWCNT/PPy was carried out using a two-step process consisting of hydrothermal treatment and surface functionalization, ensuring a straightforward and cost-effective methodology.

2.2.1. Synthesis of UzMWCNT

The fabrication of UzMWCNTs involves a sequential two-step process consisting of oxidation and reduction stages. Initially, MWCNTs undergo oxidation using a modified Hummers method. This initial stage begins by dispersing 4 g of MWCNTs and 2 g of $NaNO_3$in a 500 mL flask containing concentrated H_2SO_4 (98%). The mixture is then stirred in an ice bath for 1 hour to maintain a controlled temperature environment. Subsequently, 1 M $KMnO_4$ solution is gradually added to the suspension, ensuring the reaction temperature remains below 20°C. After removing the ice bath, the mixture is stirred at room temperature for an additional hour to facilitate the oxidation process. Next, deionized (DI) water is slowly added under vigorous stirring, followed by a 30-minute stirring period of the diluted suspension. The final step of the oxidation stage involves the addition of 20 mL of 30% H_2O_2 and 280 mL of DI water. The resulting mixture undergoes multiple cycles of washing and centrifugation with 10% HCl and deionized water until a neutral pH is achieved. Finally, vacuum drying yields the oxidized MWCNTs (O-MWCNTs) as a black powder, with a typical yield of approximately 80% based on the starting CNTs. This oxidized material then serves as the precursor for the subsequent reduction step, ultimately leading to the formation of the desired UzMWCNTs.[38]

Next, the O-MWCNTs (100 mg) were dispersed in 100 mL of water through ultrasonic treatment for 1 hour. Subsequently, 500 mg of $NaBH_4$ was gradually added to the mixture, which was then stirred for 24 hours at room temperature. The solid sample was collected after washing with ethanol and DI water and subjected to vacuum drying at 60°C, resulting in the formation of the UzMWCNT material.[66]

2.2.2. Synthesis of UzMWCNT/Polypyrrole

UzMWCNT (5wt%) suspension underwent ultrasonication for 30 minutes. Following sonication, 1 mL of PPy dispersion was introduced drop by drop into the suspensions and stirred for 30 minutes at a speed of 500 rpm. Subsequently, APS was incorporated into the mixture, and continuous stirring was maintained for another 30 minutes. To allow the polymerization reaction to progress, the mixture was stirred for 24 hours at a temperature of 0°C. After this period, black powders were collected and subjected to multiple washes with DI

DOI: 10.1039/D4MA01270D

water and ethanol to eliminate impurities. The final products were then vacuum-dried at 60°C for 24 hours.[67]

2.3. Characterization methods

The structural and morphological properties of UzMWCNT and UzMWCNT/PPy composites were comprehensively analyzed using advanced analytical techniques. The microstructure and surface morphology of the samples were investigated using scanning electron microscopy (SEM) (Nova Nano SEM 450) and high-resolution transmission electron microscopy (HRTEM) (JEM-2100). X-ray diffraction (XRD) analysis was conducted using a Rigaku XRD diffractometer, covering a wide angular range (5−80°) to identify the crystalline phases and assess the structural modifications induced by the composite formation. Raman spectroscopy, performed using a 532 nm Renishaw Raman system, further confirmed the structural characteristics, providing information on the graphitic structure and disorder in the materials. To determine the elemental composition and chemical bonding states, X-ray photoelectron spectroscopy (XPS) was carried out using a K-Alpha spectrometer (KAN9954133). The specific surface area, pore volume, and pore size distribution of the samples were determined using the Brunauer−Emmett−Teller (BET) method, conducted with a BELSORP MINI X analyser.

2.4. Supercapacitor Electrode Preparation and Testing

The preparation of supercapacitor electrodes involved coating electrode-active materials onto a nickel foam substrate using the doctor blade method. The electrode composition consisted of electrode-active material (85 wt%), polyvinylidene fluoride (PVDF, 10 wt%), and carbon black (5 wt%). To create a uniform slurry, the electrode-active material, PVDF, and carbon black were mixed with N-methyl pyrrolidine (NMP) solvent using a lab-scale mortar and pestle. This slurry was then evenly coated onto nickel foam and dried overnight in a vacuum oven at 80 °C to ensure complete solvent removal. Electrochemical performance was evaluated in a three-electrode cell configuration. The electrode-active material-coated nickel foam served as the working electrode, with platinum wire as the counter electrode and Ag/AgCl (saturated KCl) as the reference electrode. All electrochemical tests were performed using an electrochemical workstation potentiostat (CHI608E). Electrochemical evaluations included cyclic voltammetry (CV), galvanostatic charge-discharge (GCD), and electrochemical impedance spectroscopy (EIS).

View Article Online
DOI: 10.1039/D4MA01270D

2.5. Asymmetric Supercapacitor Fabrication and Testing

An asymmetric supercapacitor was fabricated to evaluate the potential application of the UzMWCNT/PPy//AC nanocomposite in energy storage devices. The device was assembled with a UzMWCNT/PPy-based positive electrode and an active carbon (AC)-based negative electrode. Aqueous 3 M KOH was used as the electrolyte, ensuring efficient ion conductivity and stability during testing. The as-fabricated UzMWCNT/PPy//AC asymmetric supercapacitor cell underwent electrochemical testing using EIS, CV, and GCD techniques.

3. Result and discussion

3.1 Structure of UzMWCNT/PPy nanocomposite

The functionalization of UzMWCNT through PPy and interfacial polymerization was analyzed using XRD, as shown in Figure 1a. The XRD patterns highlight the structural changes occurring in pristine MWCNTs, UzMWCNT, and UzMWCNT/PPy composites. In pristine MWCNTs, sharp diffraction peaks corresponding to the (002) and (100) planes indicate a well-ordered graphitic structure with a d-spacing of 0.34 nm. Upon unzipping and functionalization, the UzMWCNT sample exhibited a broader (002) peak at 26.2°, corresponding to an increased interlayer spacing of approximately 0.37 nm, likely due to the introduction of oxygen-containing functional groups and structural defects. Additionally, a broad peak at 43.3° attributed to the (100) plane suggests turbostratic disorder within the UzMWCNT framework.

The XRD spectrum of UzMWCNT/PPy demonstrates significant modifications, including a broad peak in the range of 20°–30°, centered at 26.4°, which is characteristic of pyrrole monomers. This peak appears sharper compared to pure PPy, indicating potential synergistic electronic interactions between PPy chains and the UzMWCNT substrate. The merging of diffraction peaks from UzMWCNT and PPy in the composite reflects its predominantly amorphous nature, which is favorable for supercapacitor applications. The amorphous structure enhances the interaction between the polymerized PPy and UzMWCNT, allowing for increased electrolyte ion accessibility and facilitating redox reactions. The observed reduction in crystallinity upon PPy functionalization suggests an improved electrochemical activity. This enhancement is attributed to the polymerization of PPy on the high-surface-area UzMWCNT nanosheets, enabling better ion diffusion and redox reaction kinetics.

Raman spectroscopy was utilized to analyze the chemical bonding and structural characteristics of the UzMWCNT and UzMWCNT/PPy composites, as shown in Figure 1b. The spectra reveal

View Article Online
DOI: 10.1039/D4MA01270D

the characteristic D band at 1349 cm^{-1}, indicative of structural defects, and the G band at 1584 cm^{-1}, corresponding to the in-plane stretching vibrations of sp^2-hybridized carbon atoms in both ring and chain configurations. The presence of these peaks confirms the graphitic structure of the carbon materials. For the UzMWCNT/PPy composite, a noticeable decrease in the intensity of the G band (sp^2 domains) was observed, suggesting significant modifications to the carbon structure due to functionalization with PPy. The intensity ratio (I_D/I_G) of the D peak to the G peak in UzMWCNT/PPy is higher compared to pristine UzMWCNT, indicating the introduction of abundant structural defects during the carbonization and activation processes. These structural defects enhance the surface reactivity and facilitate the interaction between UzMWCNT and PPy. The Raman spectra also confirm the successful growth of PPy onto the UzMWCNT substrate, as evidenced by the retention of characteristic signals from both components. This result aligns well with the findings from XRD analysis, corroborating the structural and compositional changes induced by the polymerization of PPy on the UzMWCNT framework. The synergistic combination of PPy and UzMWCNT enhances the composite's structural and electrochemical properties, making it a promising candidate for energy storage applications.

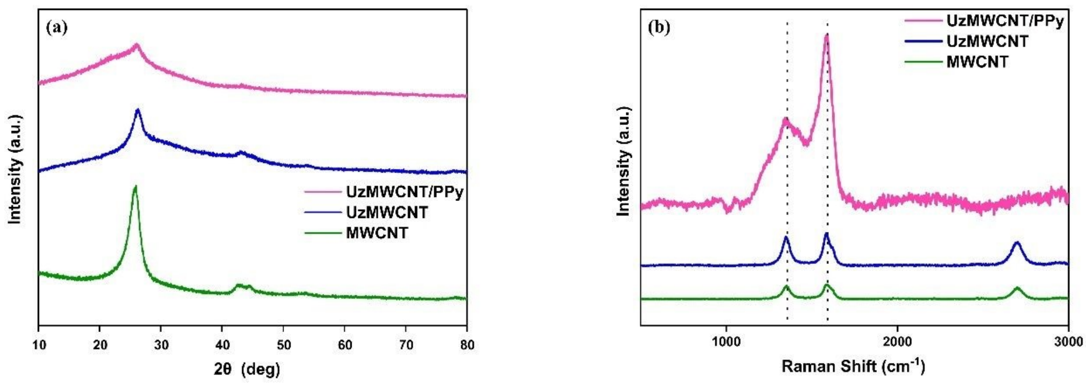

Figure 1. (a) XRD; and (b) Raman spectra of MWCNT, UzMWCNT, and the UzMWCNT/PPy nanocomposite.

XPS was performed to analyze the elemental composition and chemical bonding states in the UzMWCNT/PPy composite, as shown in Figure (2a-d). The survey spectrum (Figure 2a) reveals prominent peaks corresponding to C 1s, N 1s, and O 1s, confirming the presence of carbon, nitrogen, and oxygen elements within the composite. These elements are indicative of both the UzMWCNT and the PPy functional groups.

View Article Online
DOI: 10.1039/D4MA01270D

The high-resolution C 1s spectrum was deconvoluted into four main peaks(Figure 2b). The peak at 284.49 eV corresponds to C–C bonds, indicative of the graphitic carbon backbone. The peak at 283.94 eV represents C=C bonds, confirming the sp^2-hybridized carbon framework. Peaks at 285.09 eV and 286.34 eV are assigned to C–N/C–O and C=N/C=O bonds, respectively, highlighting the presence of oxygen and nitrogen functional groups. These peaks confirm the successful functionalization of UzMWCNT with PPy. The O 1s spectrum shows two distinct peaks at 531.49 eV and 532.49 eV, corresponding to C=O and C–O bonds,[68] respectively(Figure 2c). These oxygen-containing groups are likely introduced during the oxidation and functionalization processes, contributing to enhanced surface reactivity and improved electrochemical properties of the composite. The N 1s spectrum was deconvoluted into two main peaks at 399.59 eV and 400.09 eV, corresponding to C=N and C–NH bonds[69], respectively(Figure 2d). These nitrogen-containing bonds originate from the PPy polymer and indicate successful integration of PPy with UzMWCNT. The presence of nitrogen also enhances the pseudocapacitive behavior of the composite.

The XPS analysis confirms the successful incorporation of functional groups from both UzMWCNT and PPy, indicating the formation of a stable composite. The nitrogen and oxygen functionalities play a critical role in enhancing the electrochemical performance by increasing active sites for redox reactions and improving wettability for better interaction with electrolytes. Combining carbon materials with pseudocapacitive materials such as conducting polymers and organic moieties could help to achieve enhanced capacitance and improved rate capabilities.

View Article Online
DOI: 10.1039/D4MA01270D

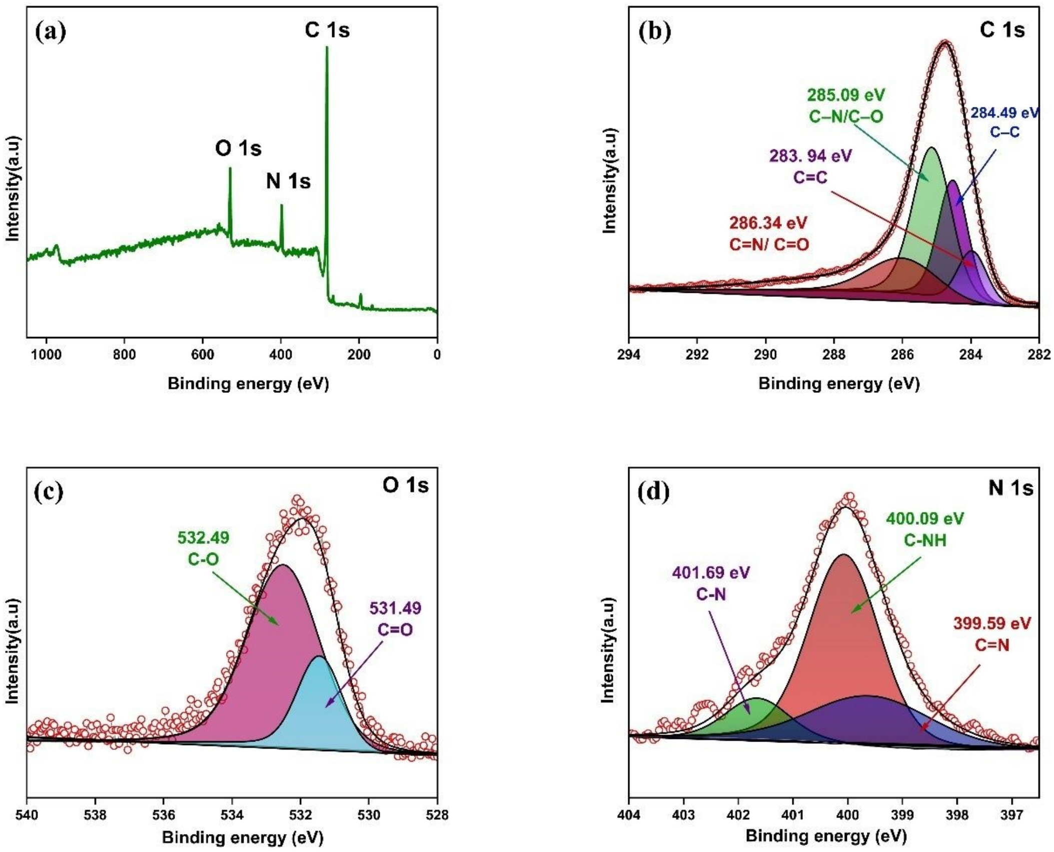

Figure 2. Deconvoluted XPS spectra of UzMWCNT/PPy: (a) survey spectra (b) C 1s, (c) O 1s, and (d) N 1s.

The surface area and pore characteristics of the synthesized nanomaterials were analyzed using N_2 adsorption-desorption isotherms and BJH pore size distribution, as shown in Figure 3. The study revealed significant changes in textural properties resulting from unzipping and functionalization processes, particularly with the introduction of PPy.

All the materials exhibited Type IV isotherms with distinct hysteresis loops at higher relative pressures, indicative of mesoporous structures. For pristine MWCNT, the BET surface area was determined to be 90 m^2/g, reflecting its baseline porosity and surface characteristics(Figure 3a). After unzipping, UzMWCNT displayed enhanced adsorption, with a BET surface area of 120 m^2/g, attributed to structural modifications and defect generation(Figure 3b). Further functionalization with PPy resulted in an increase in surface area to 168 m^2/g for UzMWCNT/PPy, highlighting the significant impact of PPy incorporation in creating additional active sites and improving pore accessibility(Figure 3c).

View Article Online
DOI: 10.1039/D4MA01270D

The BJH analysis((Figure 3d-f) confirmed the presence of mesoporous structures, with pore sizes predominantly in the range of 2–50 nm for all samples. The cumulative pore volume and distribution broadened for UzMWCNT (BET surface area 120 m²/g) compared to pristine MWCNT, indicating the introduction of additional porosity during the unzipping process. The UzMWCNT/PPy composite showed the highest cumulative pore volume and a well-defined mesoporous network, correlating with its BET surface area of 168 m²/g. The presence of large mesopores improves ionic transport, enabling the efficient formation of an electrical double layer, while the functionalization with PPy further expands the pore structure and creates interconnected networks, enhancing ion transport and electrolyte diffusion, thereby improving the interaction between Faradaic materials and the electrolyte.

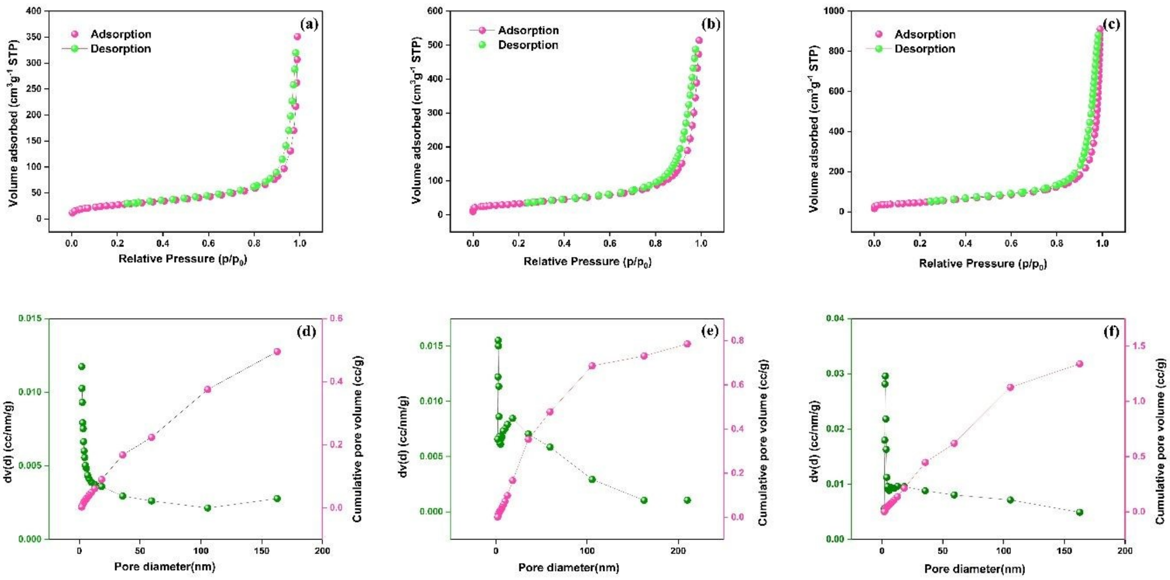

Figure 3. N_2 adsorption-desorption isotherm (a)MWCNT; (b) UzMWCNT; (c) UzMWCNT/PPy; and BJH Plot of (d) MWCNT; (e) UzMWCNT; (f) UzMWCNT/PPy

3.2 Microstructure and Surface Morphology of UzMWCNT/PPy Nanocomposite

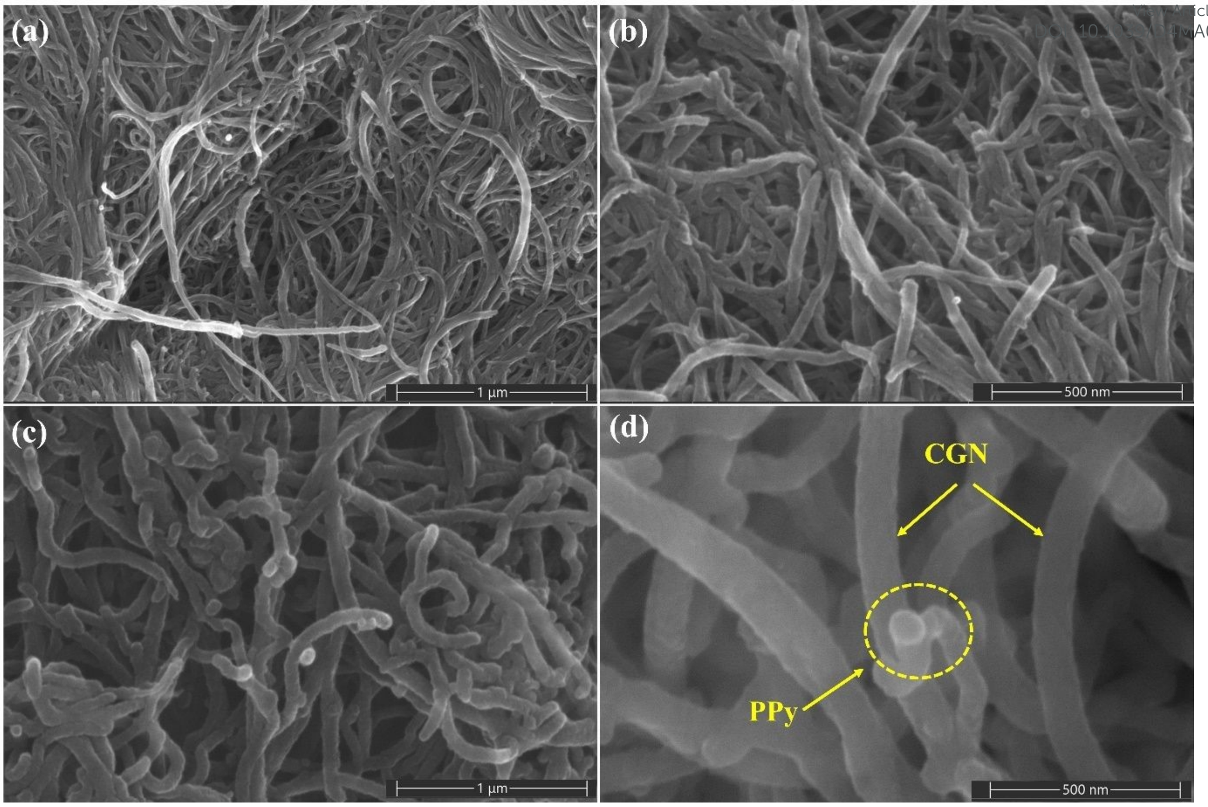

Figure 4. SEM image of (a) UzMWCNT and (b) UzMWCNT/PPy

The microstructure and surface morphology of the synthesized UzMWCNT and UzMWCNT/PPy composites were analyzed using SEM, as shown in Figures 4(a–d).

Figures 4(a) and (b) depict the SEM images of UzMWCNT, which reveal an intricate, entangled network of nanotubes with visible bundling and a porous morphology. The fine, tubular, and interconnected structure observed highlights the nanoscale features of the UzMWCNT. This morphology is particularly beneficial as it provides a high surface area, facilitating enhanced electron and ion transport-key attributes for supercapacitor electrode performance.

In Figures 4(c) and (d), the SEM images of the UzMWCNT/PPy composite show the successful integration of PPy onto the UzMWCNT framework. The porous and interconnected network structure is preserved, while the presence of PPy is clearly visible, as indicated in Figure 4d. The uniform coating of PPy enhances the overall conductivity and introduces pseudocapacitive behavior to the composite, leading to a synergistic effect. This combination of UzMWCNT's high conductivity and PPy's redox-active properties significantly improves the energy storage capacity of the material.

View Article Online
DOI: 10.1039/D4MA01270D

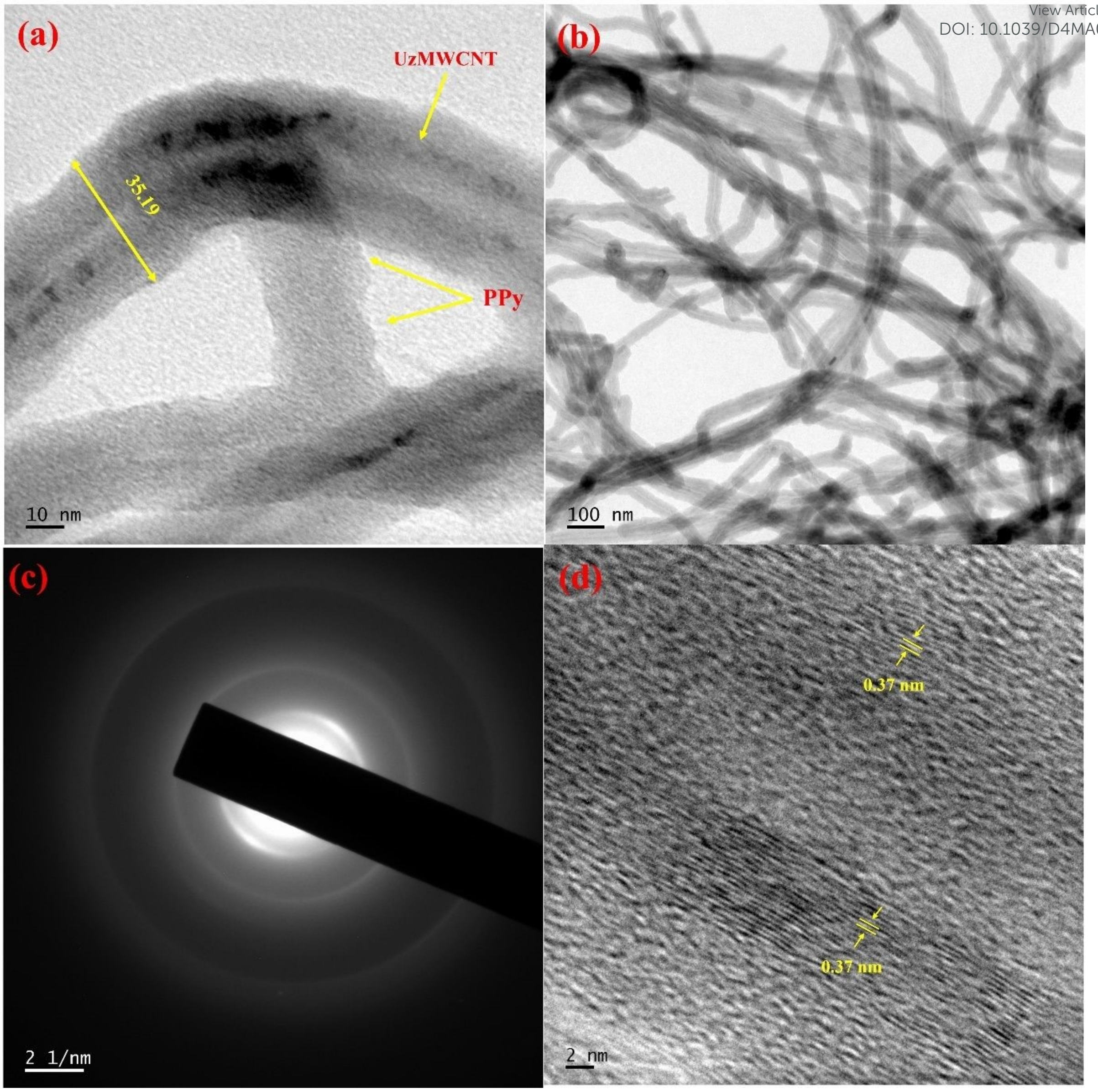

Figure 5: TEM Analysis of UzMWCNT/PPy Nanocomposite; (a,b) nanocomposite at two different magnifications (c) SAED pattern; (d) HR-TEM.

The TEM images provide detailed insights into the microstructure and polymerization behavior of PPy over UzMWCNT. As observed in Figure 5a, the UzMWCNT framework displays a well-defined tubular morphology with dimensions of approximately 35.19 nm, confirming its nanoscale structure. The uniform polymerization of PPy onto the UzMWCNT surface is evident, highlighting the successful formation of the UzMWCNT/PPy composite. The selected area electron diffraction (SAED) pattern (Figure 5c) exhibits characteristic diffraction rings, confirming the amorphous nature of the composite. In the high-resolution TEM image (Figure 5d), the interlayer spacing of 0.37 nm is distinctly visible, indicating the presence of structural modifications, which can be attributed to the unzipping and subsequent functionalization of

View Article Online
DOI: 10.1039/D4MA01270D

MWCNTs. This suggests the formation of well-integrated UzMWCNT/PPy, where the synergistic combination of the tubular carbon framework and polymerized PPy enhances conductivity and redox activity. These structural changes facilitate improved surface area and active sites for ion interaction, which are essential for enhanced electrochemical performance in energy storage applications.

3.3 Electrochemical Evaluation of UzMWCNT/PPy Composite Electrodes

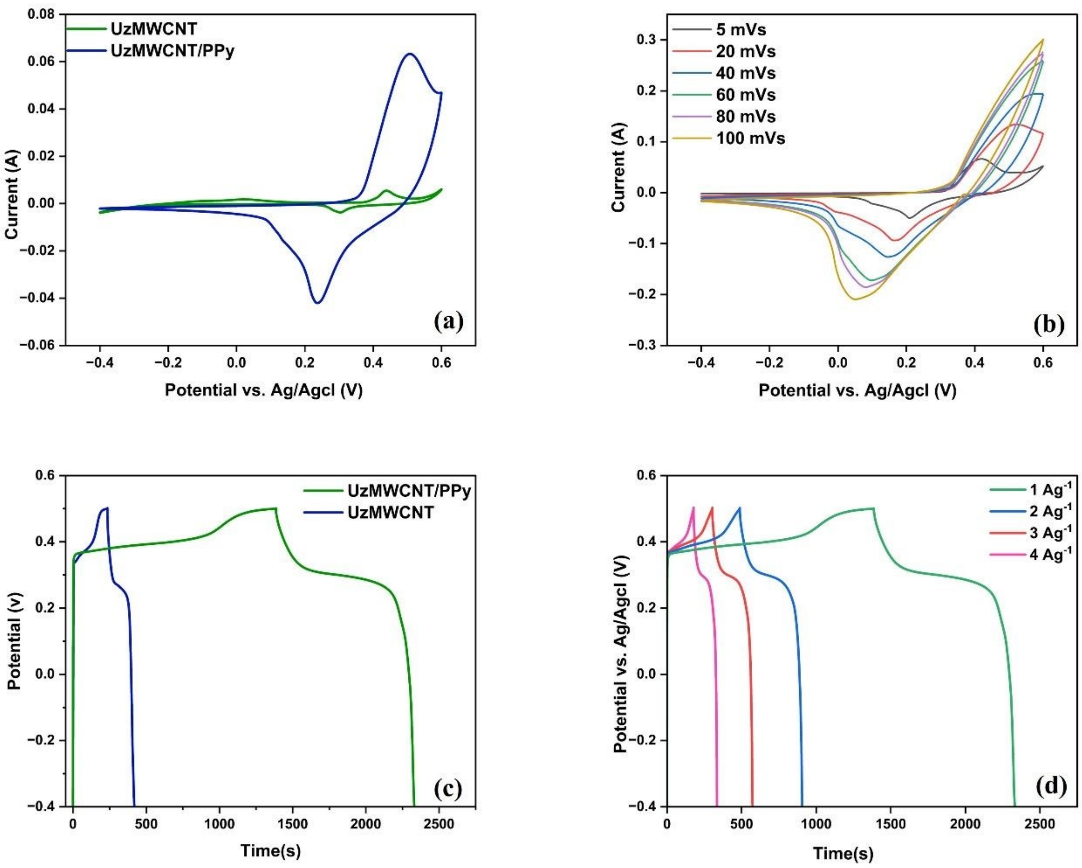

Figure 6. (a) Cyclic voltammograms of UzMWCNT and UzMWCNT/PPy nanocomposites at a fixed scan rate of 50 mV s^{-1}; (b) CV curves of UzMWCNT/PPy nanocomposite electrode at varying scan rates; (c) GCD profiles of UzMWCNT and UzMWCNT/PPy nanocomposites; (d) GCD curves of UzMWCNT/PPy nanocomposite electrodes at different current densities.

To further assess the electrochemical performance of both UzMWCNT and UzMWCNT/PPy, we conducted CV experiments shown in Figure 6. In Figure 6a the enclosed area under the CV curves is larger for UzMWCNT/PPy compared to UzMWCNT in 5mV/s. In contrast, curves clearly exhibit redox peaks, indicating that the UzMWCNT/PPy composite demonstrates pseudocapacitive behaviour. Response current rises continuously with increasing

View Article Online
DOI: 10.1039/D4MA01270D

scan rate, suggesting that ionic and electronic transport rates are fast enough at these scan rates. This emphasizes the remarkable kinetics and reversibility of the UzMWCNT/PPy combination. This indicates that the UzMWCNT/PPy composite exhibits a higher charge storage capability, attributed to the synergistic effect between the conducting PPy matrix and the UzMWCNT. The presence of well-defined redox peaks in the UzMWCNT/PPy curves confirms the occurrence of pseudocapacitive behavior, highlighting the contribution of faradaic reactions in addition to the EDLC of UzMWCNT. The enhanced redox activity can be associated with the reversible doping/dedoping processes of PPy, which further contributes to charge storage capacity.

The CV curves in Figure 6b were generated by varying the scan rates from 5 to 100 mV/s within a potential range of -0.4 to 0.6 V. Additionally, as the scan rate increases, the shape of these CV curves remains consistent, suggesting that the UzMWCNT/PPy composites possess good ionic and electronic conductivity.

Figure 6c illustrates the galvanostatic charge/discharge curves for both the UzMWCNT and UzMWCNT/PPy composites. The fact that the UzMWCNT/PPy composite exhibits the longest discharge time indicates that it possesses the highest electrochemical performance. In Figure 6b, the galvanostatic charge/discharge curves for UzMWCNT/PPy are depicted at varying current densities. The specific capacitances at different current densities were determined using Equation 1.[70] These curves exhibit a nearly linear behavior, suggesting that the composite displays good symmetry and minimal internal resistance (iR drops), supporting the notion that the unzipping process enhances electron mobility and facilitates faster charge propagation which are characteristics associated with a high-quality capacitor.[71]

$$C_{sp} = \frac{I \times \Delta t}{m \times \Delta v} \qquad (1)$$

The UzMWCNT/PPy electrode exhibits a specific capacitance of 944 F g^{-1} at a current density of 1 A g^{-1}. This high specific capacitance arises from the synergistic interaction between UzMWCNT and PPy in the nanocomposite. The large surface area of UzMWCNT nanosheets supports uniform polymerization of PPy, enhancing pseudocapacitive charge storage. A decline in specific capacitance is observed with increasing current density, which can be attributed to the limited reaction kinetics of the electrode at higher current densities. To evaluate the contribution of PPy in the composite, the specific capacitance of UzMWCNT/PPy was measured at different current densities of 1, 2, 3, and 4 A g^{-1}, yielding values of 944, 350,

View Article Online
DOI: 10.1039/D4MA01270D

205, and 157 F g⁻¹, respectively(Figure 6d). A comparison of various modified MWCNT based nanocomposite electrodes is given in Table 1.

Additionally, the non-linear curves, which match the observed redox peaks in the CV curves, provide additional evidence for the composite's pseudocapacitive nature. This suggests that UzMWCNT/PPy exhibits good charge and discharge reversibility when used as an electrode material for a supercapacitor. At the interface between the electrolyte and the active material of the electrode, electric charge can be efficiently stored and released.

Table 1 : A comparison of various modified MWCNT based nanocomposite electrodes

Electrode Material	Synthesis Method	Gravimetric Capacitance (F g^{-1})	Cycling Stability (cycles)	References
Graphene/CNT-PANI electrode	Electrodeposition	271 (0.3 A g^{-1})	10000	72
Curved graphene nanosheets	Hummers method	256 (0.3 A g^{-1})	5000	38
Graphene oxide nanoribbons	Hummers method	33 (1 A g^{-1})	Not mentioned	73
curved graphene-MnO_2	Oxidation	236 (2 A g^{-1})	1000	66
$NiSe_2$/$CoSe_2$/CNT	chemical precipitation	848 (2 A g^{-1})	1000	74
UzMWCNT/PPy	**Polymerisation**	**944 (1 A g^{-1})**	**5000**	**This work**

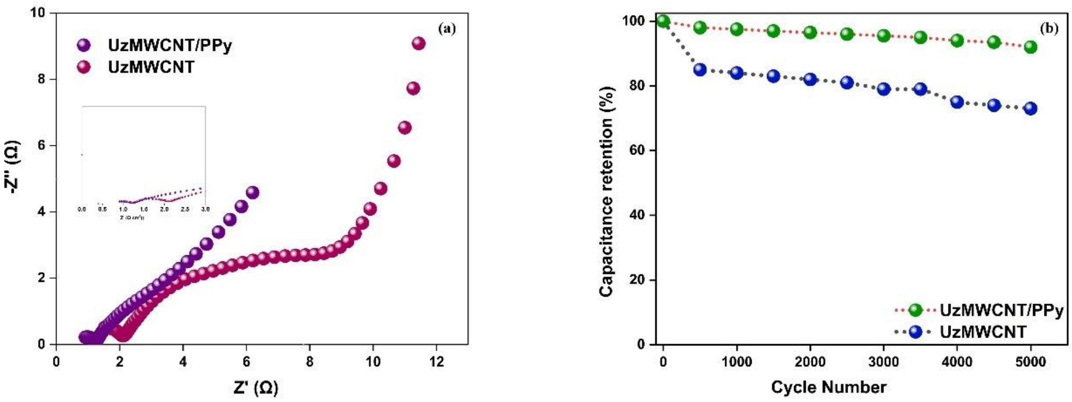

View Article Online
DOI: 10.1039/D4MA01270D

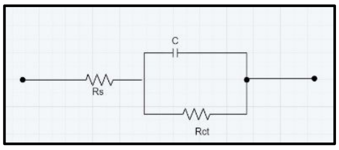

Figure 7. (a) Nyquist plot of UzMWCNT and UzMWCNT/PPy nanocomposites; (b) cycling stability of the UzMWCNT and UzMWCNT/PPy nanocomposite electrode; (c) Z-View software, employing the equivalent circuit model

In order to verify UzMWCNT/PPy's exceptional electrochemical capabilities, impedance is performed in Figure 7a . The circular arc radius of UzMWCNT/PPy composites is clearly smaller in the high-frequency range than that of pure UzMWCNT, suggesting a reduced internal resistance in the UzMWCNT/PPy composites. UzMWCNT/PPy composites show a steeper slope in the low-frequency region than PPy, which suggests quicker ion exchange during charge and discharge. The UzMWCNT's tubular hollow structure and network arrangement, which provide more electrolyte ion freedom throughout the exchange process, are responsible for this improved ion exchange. These results confirm that the electrochemical performance of supercapacitors is greatly improved by UzMWCNT/PPy composites. The increased resistance observed in UzMWCNT/PPy is primarily due to PPy's relatively poor electrical conductivity in a KOH electrolyte. However, the UzMWCNT/PPy composite demonstrates excellent rate capability. In the low-frequency region (below 1 Hz), the linear portion of the impedance curve corresponds to Warburg diffusion impedance (ZW) within the electrolyte, indicating capacitor-like behaviour. A longer ZW line suggests restricted access of electrolytic ions. At high frequencies, materials with supercapacitance properties behave like resistors, while at low frequencies, they act as capacitors.

The impedance data were analyzed using Z-View software, employing the equivalent circuit model shown in Figure 7c, which consists of a solution resistance (R_s) in series with a parallel combination of charge transfer resistance (R_{ct}) and capacitance (C)[75]. The UzMWCNT/PPy composite exhibited a lower R_{ct} value compared to pristine UzMWCNT, indicating enhanced charge transfer kinetics and reduced interfacial resistance due to the incorporation of polypyrrole, which facilitates improved electronic conductivity and ion diffusion. Furthermore, the lower R_s value observed for UzMWCNT/PPy suggests improved electrolyte accessibility and enhanced electrode-electrolyte interaction.

View Article Online
DOI: 10.1039/D4MA01270D

Cycling performance is a critical factor when evaluating supercapacitor electrodes for practical applications. In this study, the electrochemical stability of the hybrid nanocomposite was assessed at a current density of 5 Ag^{-1} , as depicted in Figure 7b. The performance of supercapacitor devices is intricately linked to the cycling stability of the electrode material. The test conditions encompassed a voltage window spanning from -0.4 to 0.6 V, with a current density of 5 Ag^{-1}. Remarkably, after 5000 cycles, the UzMWCNT/PPy electrode retained approximately 92% of its initial capacitance, indicating outstanding capacity reversibility throughout consecutive charge and discharge cycles.

It's worth noting that Polypyrrole, when used as a standalone supercapacitor electrode, often exhibits poor cycling stability. However, the incorporation of UzMWCNT sheets in the composite serves as an effective means to restrain the swelling and shrinkage of Polypyrrole during the polymerization process. This structural feature renders the hybrid material more adaptable to volumetric changes during redox reactions, contributing to its enhanced cycling stability and overall performance as a supercapacitor electrode.

3.5 UzMWCNT/PPy Asymmetric Supercapacitor Performance

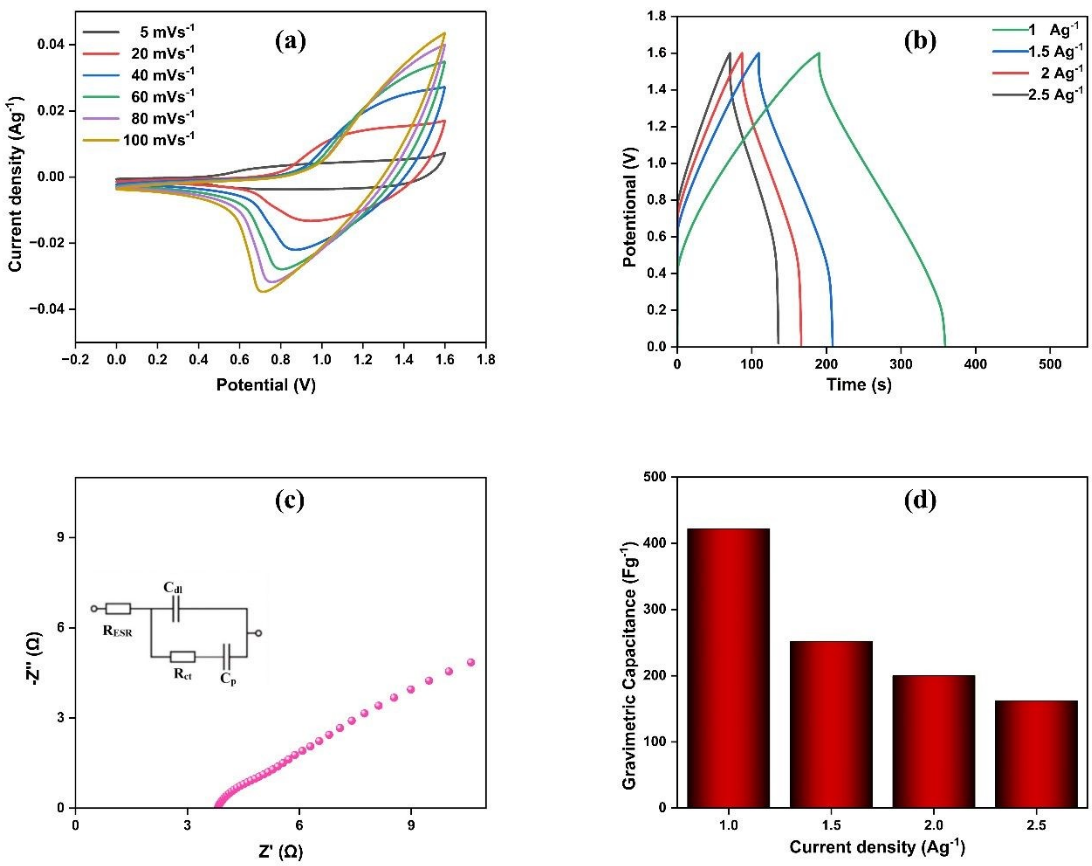

View Article Online
DOI: 10.1039/D4MA01270D

Figure 8. Electrochemical performance evaluation of the UzMWCNT/PPy//AC asymmetric supercapacitor cell (a) CV curves obtained at different scan rates; (b) GCD curves obtained at different current densities; (c) Nyquist plot of the fabricated cell; (d) Gravimetric capacitance at different current densities calculated for the cell.

To further assess the electrochemical performance of the UzMWCNT/PPy//AC composite, CV was conducted. Figure 8a displays CV curves recorded at scan rates ranging from 5 to 100 mV/s, within a potential window of 0–1.6 V. The quasi-rectangular shape of these curves indicates pseudocapacitive behavior of the UzMWCNT/PPy//AC composite. As the scan rate increases, the response current consistently rises, demonstrating that the ionic and electronic transport processes occur quickly enough to support efficient charge transfer. Additionally, the consistent shape of the CV curves across different scan rates highlights the composite's excellent ionic and electronic conductivity.

Figure 8b presents the GCD curves obtained at current densities of 1, 1.5, 2, and 2.5 Ag^{-1}. The nearly linear curves suggest good symmetry and low internal resistance (minimal iR drop), characteristics indicative of a high-performing capacitor. As the current density increases, however, a gradual deviation from the linear and symmetrical shape becomes noticeable. This nonlinear behavior further confirms the pseudocapacitive nature of the composite, aligning with the redox peaks observed in the CV curves.

EIS measurements on the UzMWCNT/PPy//AC composite (Figure 8c) show that in the high-frequency region, the semicircular arc indicates low internal resistance. In the low-frequency region, the steep slope suggests fast ion exchange during charge and discharge. The network structure of the UzMWCNT, combined with PPy, enhances the mobility of electrolyte ions during the exchange process. These findings demonstrate that the UzMWCNT/PPy//AC composite significantly improves the electrochemical performance for supercapacitors.

The bar graph shows the gravimetric capacitance of the UzMWCNT/PPy//AC composite at different current densities (1.0, 1.5, 2.0, and 2.5 Ag^{-1}). At 1.0 Ag^{-1}, the composite exhibits the highest gravimetric capacitance of approximately 400 Fg^{-1}. As the current density increases, the gravimetric capacitance gradually decreases, with around 252 Fg^{-1} at 1.5 Ag^{-1}, 200 Fg^{-1} at 2.0 Ag^{-1}, and slightly below 162 Fg^{-1} at 2.5 Ag^{-1}(Figure 8d). This reduction in capacitance at higher current densities is expected due to the limited ion diffusion and reduced utilization of the electrode's active surface. As the current density increases, ions in the electrolyte have less time to effectively reach the entire surface of the electrode, resulting in lower capacitance.

View Article Online
DOI: 10.1039/D4MA01270D

Despite this, the UzMWCNT/PPy//AC composite maintains a substantial capacitance even at higher current densities, demonstrating its good rate capability.

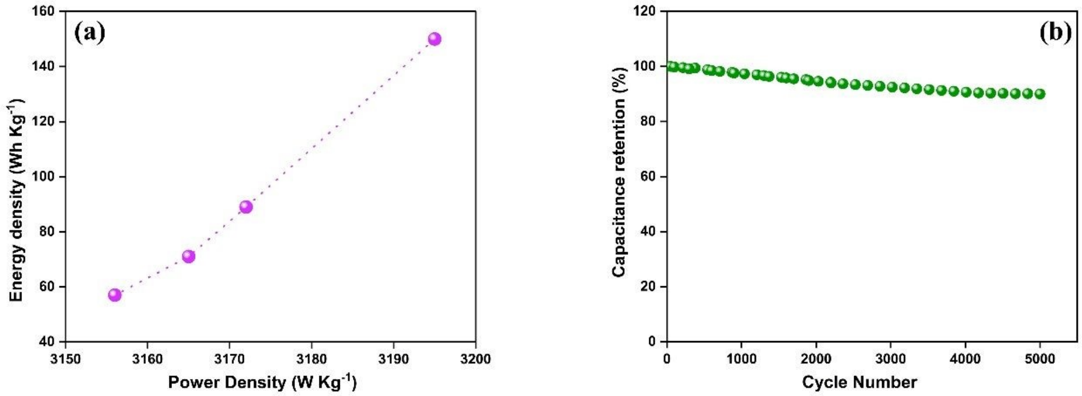

Figure 9. (a) Ragone plot for the UzMWCNT/PPy//AC asymmetric supercapacitor cell, and (b) cycling stability.

The UzMWCNT/PPy//AC composite, when employed as an electrode material, exhibited excellent charge-discharge reversibility. This performance is attributed to the efficient storage and release of charge at the interface between the active electrode material and the electrolyte, demonstrating its potential for high-performance supercapacitor applications. The energy density (E) and power density (P) of the device were further evaluated using the corresponding equations.[76–78]

$$E = \frac{c_{s_P}(\Delta v)^2}{2} \quad (2)$$

$$P = \frac{E}{\Delta t} \quad (3)$$

Energy Density is given in W hkg^{-1} and is determined using the specific capacitance (C_{sp}) and the potential shift (ΔV) squared. Power Density is represented in W kg^{-1} and is calculated using the energy (E), and time (Δ t in s).

Using the calculated formula, the specific capacitance, energy density , and power density of the UzMWCNT/PPy//AC composite at varying current densities are shown in Figure 9a. The fabricated asymmetric supercapacitor cell demonstrates excellent capacitive behavior, achieving an energy density of 150 Wh kg^{-1} with a corresponding power density of 3195 W kg^{-1}. Table 2 summarizes recent studies on supercapacitor electrodes utilizing PPy and CNT

View Article Online
DOI: 10.1039/D4MA01270D

composites, highlighting their fabrication methods and corresponding energy and power densities.

The cycling stability of the fabricated cell was evaluated over 5000 charge-discharge cycles at a current density of 5 Ag^{-1}(Figure 9b). The cell exhibited exceptional performance, maintaining 95% of its initial capacitance, which highlights its durability and the stability of the electrochemical system.

Table 2 : Performance Comparison of PPy/CNT Supercapacitor Electrodes

Supercapacitor Electrodes	**Method**	**Power Density (WKg^{-1})**	**Energy Density ($WhKg^{-1}$)**	**Ref.**
Polypyrrole/Carbon Nanotube	Electrodeposition	402	31.2	[79]
Polypyrrole/Carbon Nanotube	Chemical Vapor Deposition	1051	3.57	[80]
Copper Doped PPy/MWCNT	Oxidative Polymerization	19.89	4479	[81]
Polypyrrole/Graphene Oxide/ Multi-Walled Carbon Nanotubes	Electropolymerization	441.24	40.45	[82]
CO3o4@Polypyrrole/Mwcnt	Hydrothermal Process.	1500	84.58	[83]
UzMWCNT/PPy	**Modified Hummers Process**	**3195**	**150**	**This work**

Conclusion

The unzipped MWCNT/polypyrrole (UzMWCNT/PPy) composite electrodes demonstrated exceptional electrochemical performance, making them a promising candidate for high-performance supercapacitor applications. The novel unzipping method, achieved through a modified Hummers process followed by reduction, effectively transformed multi-walled carbon nanotubes into UzMWCNT with enhanced structural and functional properties. The hybrid UzMWCNT/PPy composite exhibited a high specific capacitance of 944 F g^{-1} at 1 A g^{-1}, excellent cycling stability with 92% capacitance retention after 5000 cycles, and impressive gravimetric capacitance retention of approximately 95% in an asymmetric configuration with active carbon electrodes. The synergistic integration of UzMWCNT and PPy enabled superior pseudocapacitive behavior, improved ion transport, and enhanced charge storage capabilities. The increased surface area, mesoporous structure, and tailored conductivity of the composite contributed to its remarkable energy storage performance. These findings highlight the potential of UzMWCNT/PPy composites in developing next-generation energy storage devices with high energy density, excellent cyclic stability, and robust durability.

Acknowledgments

Centre for Research, CHRIST University, for the support provided for this research work.

Reference

1. Lebaschi S, Hekmati M, Veisi H. Green synthesis of palladium nanoparticles mediated by black tea leaves (Camellia sinensis) extract: Catalytic activity in the reduction of 4-nitrophenol and Suzuki-Miyaura coupling reaction under ligand-free conditions. *J Colloid Interface Sci*. 2017;485:223-231. doi:10.1016/j.jcis.2016.09.027

2. Han K, Liu Y, Huang H, Gong Q, Zhang Z, Zhou G. Tremella-like NiO microspheres embedded with fish-scale-like polypyrrole for high-performance asymmetric supercapacitor. *RSC Adv*. 2019;9(38):21608-21615. doi:10.1039/c9ra03046h

3. Simon S, James N, Sreeja PB. Water hyacinth-poly(3,4-Ethylenedioxythiophene) composite as a facile electrode for supercapacitor application. *Mater Today Proc*. 2023;(August 2023). doi:10.1016/j.matpr.2023.10.068

4. Bangera DN, Sudhakar YN, Nazareth RA. Concrete-based energy storage: exploring electrode and electrolyte enhancements. *RSC Adv*. 2024;14(39):28854-28880. doi:10.1039/d4ra04812a

5. Beyers I, Bensmann A, Hanke-Rauschenbach R. Ragone plots revisited: A review of methodology and application across energy storage technologies. *J Energy Storage*. 2023;73(PD):109097. doi:10.1016/j.est.2023.109097

6. Liu Y, Jiang SP, Shao Z. Intercalation pseudocapacitance in electrochemical energy storage: recent advances in fundamental understanding and materials development. *Mater Today Adv*. 2020;7:100072. doi:10.1016/j.mtadv.2020.100072

View Article Online
DOI: 10.1039/D4MA01270D

7. Zhong M, Zhang M, Li X. Carbon nanomaterials and their composites for supercapacitors. *Carbon Energy*. 2022;4(5):950-985. doi:10.1002/cey2.219

8. Nandi D, Mohan VB, Bhowmick AK, Bhattacharyya D. Metal/metal oxide decorated graphene synthesis and application as supercapacitor: a review. *J Mater Sci*. 2020;55(15):6375-6400. doi:10.1007/s10853-020-04475-z

9. Kumar R, Joanni E, Sahoo S, et al. An overview of recent progress in nanostructured carbon-based supercapacitor electrodes: From zero to bi-dimensional materials. *Carbon N Y*. 2022;193:298-338. doi:10.1016/j.carbon.2022.03.023

10. Wang L, Yang G, Peng S, Wang J, Yan W, Ramakrishna S. One-dimensional nanomaterials toward electrochemical sodium-ion storage applications via electrospinning. *Energy Storage Mater*. 2020;25:443-476. doi:10.1016/J.ENSM.2019.09.036

11. Adedoja OS, Sadiku ER, Hamam Y. An Overview of the Emerging Technologies and Composite Materials for Supercapacitors in Energy Storage Applications. *Polymers (Basel)*. 2023;15(10):1-32. doi:10.3390/polym15102272

12. Kamila S, Jena BK, Basu S. Advances in Electrochemical Energy Storaage Device: Supercapacitor. *Photocond Photocond Mater Fundam Energy Storage*. Published online 2021:119-147. doi:10.1002/9781119555599.ch4

13. Mossali E, Picone N, Gentilini L, Rodrìguez O, Pérez JM, Colledani M. Lithium-ion batteries towards circular economy: A literature review of opportunities and issues of recycling treatments. *J Environ Manage*. 2020;264. doi:10.1016/j.jenvman.2020.110500

14. Hemmati R, Saboori H. Emergence of hybrid energy storage systems in renewable energy and transport applications – A review. *Renew Sustain Energy Rev*. 2016;65:11-23. doi:10.1016/j.rser.2016.06.029

15. Mondal R, Mishra NK, Maiyalagan T, Gupta A, Singh P. La1-xK xFeO3-δ: An Anion Intercalative Pseudocapacitive Electrode for Supercapacitor Application. *ACS Omega*. 2021;6(45):30488-30498. doi:10.1021/acsomega.1c03902

16. Ma C, Bai J, Demir M, Hu X, Liu S, Wang L. Water chestnut shell-derived N/S-doped porous carbons and their applications in CO2 adsorption and supercapacitor. *Fuel*.

View Article Online
DOI: 10.1039/D4MA01270D

2022;326:125119. doi:10.1016/J.FUEL.2022.125119

17. Farma R, Tania Y, Apriyani I. Conversion of hazelnut seed shell biomass into porous activated carbon with KOH and CO2 activation for supercapacitors. *Mater Today Proc*. 2023;87:51-56. doi:10.1016/J.MATPR.2023.02.099

18. Lobato-Peralta DR, Okoye PU, Alegre C. A review on carbon materials for electrochemical energy storage applications: State of the art, implementation, and synergy with metallic compounds for supercapacitor and battery electrodes. *J Power Sources*. 2024;617(July). doi:10.1016/j.jpowsour.2024.235140

19. Singha DK, Mohanty RI, Bhanja P, Jena BK. Metal-organic framework and graphene composites: advanced materials for electrochemical supercapacitor applications. *Mater Adv*. 2023;4(20):4679-4706. doi:10.1039/d3ma00523b

20. Huang M, Wang L, Chen S, et al. Highly flexible all-solid-state cable-type supercapacitors based on Cu/reduced graphene oxide/manganese dioxide fibers. *RSC Adv*. 2017;7(17):10092-10099. doi:10.1039/c6ra28117f

21. Balaji TE, Tanaya Das H, Maiyalagan T. Recent Trends in Bimetallic Oxides and Their Composites as Electrode Materials for Supercapacitor Applications. *ChemElectroChem*. 2021;8(10):1723-1746. doi:10.1002/celc.202100098

22. Pour GB, Ashourifar H, Aval LF, Solaymani S. CNTs-Supercapacitors: A Review of Electrode Nanocomposites Based on CNTs, Graphene, Metals, and Polymers. *Symmetry (Basel)*. 2023;15(6):1-16. doi:10.3390/sym15061179

23. Jasna M, Muraleedharan Pillai M, Abhilash A, Midhun PS, Jayalekshmi S, Jayaraj MK. Polyaniline wrapped carbon nanotube/exfoliated MoS2 nanosheet composite as a promising electrode for high power supercapacitors. *Carbon Trends*. 2022;7:100154. doi:10.1016/J.CARTRE.2022.100154

24. Murjani BO, Kadu PS, Bansod M, Vaidya SS, Yadav MD. Carbon nanotubes in biomedical applications: current status, promises, and challenges. *Carbon Lett*. 2022;32(5):1207-1226. doi:10.1007/s42823-022-00364-4

25. Abitkar SB, Jadhav PR, Tarwal NL, Moholkar A V., Patil CE. A facile synthesis of α-Ni(OH)2-CNT composite films for supercapacitor application. *Adv Powder Technol*. 2019;30(10):2285-2292. doi:10.1016/j.apt.2019.07.008

26. Ouyang J. Applications of carbon nanotubes and graphene for third-generation solar cells and fuel cells. *Nano Mater Sci*. 2019;1(2):77-90. doi:10.1016/j.nanoms.2019.03.004

27. Snook GA, Kao P, Best AS. Conducting-polymer-based supercapacitor devices and electrodes. *J Power Sources*. 2011;196(1):1-12. doi:10.1016/J.JPOWSOUR.2010.06.084

28. Zhu S, Ni J, Li Y. Carbon nanotube-based electrodes for flexible supercapacitors. *Nano Res*. 2020;13(7):1825-1841. doi:10.1007/s12274-020-2729-5

29. Lv P, Meng Y, Song L, Pang H, Liu W. A self-supported electrode for supercapacitors based on nanocellulose/multi-walled carbon nanotubes/polypyrrole composite. *RSC Adv*. 2020;11(2):1109-1114. doi:10.1039/d0ra08040c

30. Lin CL, Li JW, Chen YF, Chen JX, Cheng CC, Chiu CW. Graphene Nanoplatelet/Multiwalled Carbon Nanotube/Polypyrrole Hybrid Fillers in Polyurethane Nanohybrids with 3D Conductive Networks for EMI Shielding. *ACS Omega*. 2022;7(49):45697-45707. doi:10.1021/acsomega.2c06613

31. Khare R, Shinde DB, Bansode S, et al. Graphene nanoribbons as prospective field emitter. *Appl Phys Lett*. 2015;106(2). doi:10.1063/1.4905473

32. Parayangattil Jyothibasu J, Chen MZ, Lee RH. Polypyrrole/Carbon Nanotube Freestanding Electrode with Excellent Electrochemical Properties for High-Performance All-Solid-State Supercapacitors. *ACS Omega*. 2020;5(12):6441-6451. doi:10.1021/acsomega.9b04029

33. Rahman Khan MM, Rumon MMH. Recent Progress on the Synthesis, Morphological Topography, and Battery Applications of Polypyrrole-Based Nanocomposites. *Polymers (Basel)*. 2024;16(23). doi:10.3390/polym16233277

34. Mahajan P, Sardana S, Mahajan A. 1D graphene nanoribbons-mediated defect engineering in 2D MXene for high-performance supercapacitors. *Appl Phys Lett*. 2024;124(11). doi:10.1063/5.0179060

35. Pan H, Li J, Feng YP. Carbon nanotubes for supercapacitor. *Nanoscale Res Lett*. 2010;5(3):654-668. doi:10.1007/s11671-009-9508-2

36. Aphale A, Maisuria K, Mahapatra MK, Santiago A, Singh P, Patra P. Hybrid

Electrodes by In-Situ Integration of Graphene and Carbon-Nanotubes in Polypyrrole for Supercapacitors OPEN. *Nat Publ Gr*. 2015;5:14445. doi:10.1038/srep14445

37. Geim AK, Novoselov KS. *The Rise of Graphene*. www.nature.com/naturematerials

38. Wang H, Wang Y, Hu Z, Wang X. Cutting and unzipping multiwalled carbon nanotubes into curved graphene nanosheets and their enhanced supercapacitor performance. *ACS Appl Mater Interfaces*. 2012;4(12):6827-6834. doi:10.1021/am302000z

39. Abdalla S, Al-Marzouki F, Al-Ghamdi AA, Abdel-Daiem A. Different Technical Applications of Carbon Nanotubes. *Nanoscale Res Lett*. 2015;10(1). doi:10.1186/s11671-015-1056-3

40. Zhang B, Kang F, Tarascon JM, Kim JK. Recent advances in electrospun carbon nanofibers and their application in electrochemical energy storage. *Prog Mater Sci*. 2016;76:319-380. doi:10.1016/j.pmatsci.2015.08.002

41. Michael F. L.; De Volder, Sameh H.; Tawfick, Ray H.; Baughman, A. John ;Hart. Carbon Nanotubes: Present and Future Commercial Applications. *Science (80-)*. 2013;339(6119):535-539. http://science.sciencemag.org/content/339/6119/535?sid=599bece0-48b5-4fcc-9d21-5e29be89422c

42. Otowa T, Tanibata R, Itoh M. Production and adsorption characteristics of MAXSORB: High-surface-area active carbon. *Gas Sep Purif*. 1993;7(4):241-245. doi:10.1016/0950-4214(93)80024-Q

43. Moriau LJ, Bele M, Vižintin A, et al. Synthesis and Advanced Electrochemical Characterization of Multifunctional Electrocatalytic Composite for Unitized Regenerative Fuel Cell. *ACS Catal*. 2019;9(12):11468-11483. doi:10.1021/acscatal.9b03385

44. Fisher RA, Watt MR, Jud Ready W. Functionalized Carbon Nanotube Supercapacitor Electrodes: A Review on Pseudocapacitive Materials. *ECS J Solid State Sci Technol*. 2013;2(10):M3170-M3177. doi:10.1149/2.017310jss

45. Shahriary L, Athawale A a. Graphene Oxide Synthesized by using Modified Hummers Approach. *Int J Renew Energy Environ Eng*. 2014;02(01):58-63.

View Article Online
DOI: 10.1039/D4MA01270D

46. Tan RKL, Reeves SP, Hashemi N, et al. Graphene as a flexible electrode: Review of fabrication approaches. *J Mater Chem A*. 2017;5(34):17777-17803. doi:10.1039/c7ta05759h

47. Shi Y, Pan L, Liu B, et al. Nanostructured conductive polypyrrole hydrogels as high-performance, flexible supercapacitor electrodes. *J Mater Chem A*. 2014;2(17):6086-6091. doi:10.1039/c4ta00484a

48. Reich S, Burgard M, Langner M, et al. ARTICLE Polymer nanofibre composite nonwovens with metal-like electrical conductivity. 2018;2:5. doi:10.1038/s41528-017-0018-5

49. Xue J, Sun Q, Zhang Y, Mao W, Li F, Yin C. Preparation of a Polypyrrole/Graphene Oxide Composite Electrode by Electrochemical Codeposition for Capacitor Deionization. *Cite This ACS Omega*. 2020;5:10995-11004. doi:10.1021/acsomega.0c00817

50. Meng Q, Cai K, Chen Y, Chen L. Research progress on conducting polymer based supercapacitor electrode materials. *Nano Energy*. 2017;36:268-285. doi:10.1016/J.NANOEN.2017.04.040

51. Thines KR, Abdullah EC, Mubarak NM, Ruthiraan M. In-situ polymerization of magnetic biochar – polypyrrole composite: A novel application in supercapacitor. *Biomass and Bioenergy*. 2017;98:95-111. doi:10.1016/j.biombioe.2017.01.019

52. Moyseowicz A, Pajak K, Gajewska K, Gryglewicz G. Synthesis of polypyrrole/reduced graphene oxide hybrids via hydrothermal treatment for energy storage applications. *Materials (Basel)*. 2020;13(10). doi:10.3390/ma13102273

53. Jyothibasu JP, Chen MZ, Tien YC, et al. V2o5/carbon nanotube/polypyrrole based freestanding negative electrodes for high-performance supercapacitors. *Catalysts*. 2021;11(8):1-15. doi:10.3390/catal11080980

54. Cong Y, Liu S, Chen H. Fabrication of Conductive Polypyrrole Nanofibers by Electrospinning. *J Nanomater*. 2013;2013. doi:10.1155/2013/148347

55. Yussuf A, Al-Saleh M, Al-Enezi S, Abraham G. Synthesis and Characterization of Conductive Polypyrrole: The Influence of the Oxidants and Monomer on the Electrical, Thermal, and Morphological Properties. *Int J Polym Sci*. 2018;2018.

View Article Online
DOI: 10.1039/D4MA01270D

doi:10.1155/2018/4191747

56. Cortijo A, Vozmediano MAH. Electronic properties of curved graphene sheets. *Epl*. 2007;77(4):1-4. doi:10.1209/0295-5075/77/47002

57. Siwal SS, Zhang Q, Devi N, Thakur VK. Carbon-based polymer nanocomposite for high-performance energy storage applications. *Polymers (Basel)*. 2020;12(3):1-30. doi:10.3390/polym12030505

58. Jang J, Yoon H. Facile fabrication of polypyrrole nanotubes using reverse microemulsion polymerization. *Chem Commun*. 2003;3(6):720-721. doi:10.1039/b211716a

59. Laforgue A. All-textile flexible supercapacitors using electrospun poly(3,4-ethylenedioxythiophene) nanofibers. *J Power Sources*. 2011;196(1):559-564. doi:10.1016/J.JPOWSOUR.2010.07.007

60. Zhang J, Zhao XS. Conducting polymers directly coated on reduced graphene oxide sheets as high-performance supercapacitor electrodes. *J Phys Chem C*. 2012;116(9):5420-5426. doi:10.1021/jp211474e

61. Adriyani TR, Ensafi AA, Rezaei B. Flexible and sewable electrode based on Ni-Co@PANI-salphen composite-coated on textiles for wearable supercapacitor. *Sci Rep*. 2023;13(1):1-13. doi:10.1038/s41598-023-47067-y

62. Tran XT, Park SS, Song S, et al. Electroconductive performance of polypyrrole/reduced graphene oxide/carbon nanotube composites synthesized via in situ oxidative polymerization. *J Mater Sci*. 2019;54(4):3156-3173. doi:10.1007/s10853-018-3043-4

63. Pattanayak P, Papiya F, Kumar V, Singh A, Kundu PP. Performance evaluation of poly(aniline-co-pyrrole) wrapped titanium dioxide nanocomposite as an air-cathode catalyst material for microbial fuel cell. *Mater Sci Eng C*. 2021;118. doi:10.1016/j.msec.2020.111492

64. An KH, Jeon KK, Heo JK, Lim SC, Bae DJ, Lee YH. High-Capacitance Supercapacitor Using a Nanocomposite Electrode of Single-Walled Carbon Nanotube and Polypyrrole. *J Electrochem Soc*. 2002;149(8):A1058. doi:10.1149/1.1491235

65. Cheng Q, Tang J, Ma J, Zhang H, Shinya N, Qin LC. Graphene and carbon nanotube

composite electrodes for supercapacitors with ultra-high energy density. *Phys Chem Chem Phys*. 2011;13(39):17615-17624. doi:10.1039/c1cp21910c

66. Li XY, Wang Q, Wang HW. Conversion of carbon nanotubes into curved graphene with improved capacitance. *Xinxing Tan Cailiao/New Carbon Mater*. 2021;36(4):835-842. doi:10.1016/S1872-5805(21)60086-0

67. Zhu Y, Shi K, Zhitomirsky I. q. *J Power Sources*. 2014;268(January 2018):233-239. doi:10.1016/j.jpowsour.2014.06.046

68. Li C, Zhang X, Qu G, et al. Highly Reversible Zn Metal Anode Securing by Functional Electrolyte Modulation. *Adv Energy Mater*. 2024;2400872:1-10. doi:10.1002/aenm.202400872

69. Zhu J, Lu XF, Luan D, Lou XW. Metal–Organic Frameworks Derived Carbon-Supported Metal Electrocatalysts for Energy-Related Reduction Reactions. *Angew Chemie - Int Ed*. 2024;202408846. doi:10.1002/anie.202408846

70. Hajare R, Kempahanumakkagaari S, Ramakrishnappa T, Saniya A, Sourav K, Amrutha A. Study of advances in carbon composites as electrodes for supercapacitors. *Mater Today Proc*. 2022;49:650-659. doi:10.1016/J.MATPR.2021.05.164

71. Shah SS, Cevik E, Aziz MA, Qahtan TF, Bozkurt A, Yamani ZH. Jute Sticks Derived and Commercially Available Activated Carbons for Symmetric Supercapacitors with Bio-electrolyte: A Comparative Study. *Synth Met*. 2021;277(January). doi:10.1016/j.synthmet.2021.116765

72. Cheng Q, Tang J, Shinya N, Qin LC. Polyaniline modified graphene and carbon nanotube composite electrode for asymmetric supercapacitors of high energy density. *J Power Sources*. 2013;241:423-428. doi:10.1016/j.jpowsour.2013.04.105

73. Fathi M, Saghafi M, Mahboubi F. Graphene oxide nanoribbons and their applications in supercapacitors. 2014;47(2):71-76.

74. Zheng J, Bai X. Preparation of Ni-Co PBA-derived beaded NiSe2/CoSe2/CNT for high-performance supercapacitors. *J Alloys Compd*. 2023;944:169110. doi:10.1016/J.JALLCOM.2023.169110

75. Li N, Zhang X, Zhao S, et al. Amorphous nickel borate nanosheets as cathode material with high capacity and better cycling performance for zinc ion battery. *Chinese Chem*

Lett. 2023;34(6):38-41. doi:10.1016/j.cclet.2022.07.012

76. Thubsuang U, Laebang S, Manmuanpom N, Wongkasemjit S, Chaisuwan T. Tuning pore characteristics of porous carbon monoliths prepared from rubber wood waste treated with H3PO4 or NaOH and their potential as supercapacitor electrode materials. *J Mater Sci*. 2017;52(11):6837-6855. doi:10.1007/s10853-017-0922-z

77. Ganganboina AB, Chowdhury AD, Doong R an. Nano assembly of N-doped graphene quantum dots anchored Fe3O4/halloysite nanotubes for high performance supercapacitor. *Electrochim Acta*. 2017;245:912-923. doi:10.1016/j.electacta.2017.06.002

78. Jeyaranjan A, Sakthivel TS, Neal CJ, Seal S. Scalable ternary hierarchical microspheres composed of PANI/ rGO/CeO2 for high performance supercapacitor applications. *Carbon N Y*. 2019;151:192-202. doi:10.1016/j.carbon.2019.05.043

79. Xu R, Wei J, Guo F, et al. Highly conductive, twistable and bendable polypyrrole-carbon nanotube fiber for efficient supercapacitor electrodes. *RSC Adv*. 2015;5(28):22015-22021. doi:10.1039/c5ra01917f

80. Lee H, Kim H, Cho MS, Choi J, Lee Y. Fabrication of polypyrrole (PPy)/carbon nanotube (CNT) composite electrode on ceramic fabric for supercapacitor applications. *Electrochim Acta*. 2011;56(22):7460-7466. doi:10.1016/j.electacta.2011.06.113

81. Mounika K, Anupama B, Pragathi J, Gyanakumari C. Journal of scientific research. *J Sci Res*. 2010;2:513-524. doi:10.3329/jsr.v2i3.4899

82. Mohd Abdah MAA, Mohd Razali NS, Lim PT, Kulandaivalu S, Sulaiman Y. One-step potentiostatic electrodeposition of polypyrrole/graphene oxide/multi-walled carbon nanotubes ternary nanocomposite for supercapacitor. *Mater Chem Phys*. 2018;219(June):120-128. doi:10.1016/j.matchemphys.2018.08.018

83. Ramesh S, Haldorai Y, Kim HS, Kim JH. A nanocrystalline Co3O4@polypyrrole/MWCNT hybrid nanocomposite for high performance electrochemical supercapacitors. *RSC Adv*. 2017;7(58):36833-36843. doi:10.1039/c7ra06093a

View Article Online
DOI: 10.1039/D4MA01270D

View Article Online
DOI: 10.1039/D4MA01270D

Unzipped MWCNT/Polypyrrole Hybrid Composites: A Pathway to High-Performance Asymmetric Supercapacitors

Shilpa Simon[a], Letcy V Theresa[a], Sreeja P B[a]*

[a] Department of Chemistry, Christ University, Bengaluru 560029, IN
*Corresponding Author

E-mail: sreeja.pb@christuniversity.in,

https://orcid.org/**0000-0002-2106-7867**

Data Availability Statement

The data that support the findings of this study are available from the corresponding author upon reasonable request.